Journal of Hazardous Materials 431 (2022) 128615

Contents lists available at ScienceDirect

Journal of Hazardous Materials

journal homepage: www.elsevier.com/locate/jhazmat

Systematic developmental toxicity assessment of a structurally diverse library of PFAS in zebrafish

Lisa Truong [a], Yvonne Rericha [a], Preethi Thunga [b], Skylar Marvel [b], Dylan Wallis [b], Michael T. Simonich [a], Jennifer A. Field [c], Dunping Cao [c], David M. Reif [b], Robyn L. Tanguay [b,*]

[a] Department of Environmental and Molecular Toxicology, the Sinnhuber Aquatic Research Laboratory, and the Environmental Health Sciences Center at Oregon State University, Corvallis, OR, USA
[b] Bioinformatics Research Center, Department of Biological Sciences, North Carolina State University, Raleigh, NC, USA
[c] Department of Environmental and Molecular Toxicology, Department of Chemistry at Oregon State University, Corvallis, OR, USA

HIGHLIGHTS

- Exposure to 49 of 139 PFAS affected zebrafish development.
- PFDA was the most developmentally toxic.
- Volatility (out of 5 physicochemical properties) correlated with PFAS bioactivity.
- Six of 36 super chemotypes were enriched in PFAS that induced developmental toxicity.

GRAPHICAL ABSTRACT

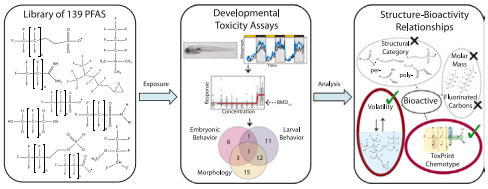

ARTICLE INFO

Editor: Jörg Rinklebe

Keywords:
PFAS
Developmental toxicity
Structure-activity relationship
Abnormal behavior
Zebrafish

ABSTRACT

Per- and polyfluoroalkyl substances (PFAS) are a class of widely used chemicals with limited human health effects data relative to the diversity of structures manufactured. To help fill this data gap, an extensive in vivo developmental toxicity screen was performed on 139 PFAS provided by the US EPA. Dechorionated embryonic zebrafish were exposed to 10 nominal water concentrations of PFAS (0.015–100 μM) from 6 to 120 h post-fertilization (hpf). The embryos were assayed for embryonic photomotor response (EPR), larval photomotor response (LPR), and 13 morphological endpoints. A total of 49 PFAS (35%) were bioactive in one or more assays (11 altered EPR, 25 altered LPR, and 31 altered morphology). Perfluorooctanesulfonamide (FOSA) was the only structure that was bioactive in all 3 assays, while Perfluorodecanoic acid (PFDA) was the most potent teratogen. Low PFAS volatility was associated with developmental toxicity ($p < 0.01$), but no association was detected between bioactivity and five other physicochemical parameters. The bioactive PFAS were enriched for 6 supergroup chemotypes. The results illustrate the power of a multi-dimensional in vivo platform to assess the developmental (neuro)toxicity of diverse PFAS and in the acceleration of PFAS safety research.

Abbreviations: PFAS, Per- and polyfluoroalkyl substances; hpf, Hours post fertilization; EPR, Embryonic Photomotor Response; LPR, Larval Photomotor Response; EM, Embryo medium; DMSO, Dimethyl sulfoxide; EC_{80}, Effective concentration at which 80% of the exposure group experiences an effect; BMD, Benchmark Dose; LIMS, Laboratory Information Management System; CT, Chemotype.

* Correspondence to: Department of Environmental and Molecular Toxicology, the Sinnhuber Aquatic Research Laboratory, 28645 East Highway 34, Oregon State University, Corvallis, OR 97333, USA.
E-mail address: Robyn.Tanguay@oregonstate.edu (R.L. Tanguay).

https://doi.org/10.1016/j.jhazmat.2022.128615
Received 8 January 2022; Received in revised form 20 February 2022; Accepted 28 February 2022
Available online 2 March 2022

1. Introduction

There are thousands of per- and polyfluoroalkyl substances (PFAS) on the global market. The exact number in use is not precisely known. But their heavy use for water- and dirt-repellents, lubricants, wetting agents, and other non-stick consumer products makes PFAS among the most widely used chemical classes in the world. Unfortunately, the environmental stability of the C-F bond also means that PFAS may now be the most ubiquitous human-made contaminant on earth (U.S. Food & Drug Administration, 2021). The persistent nature of the C-F bond has raised global concerns that the biosphere may be perpetually exposed to these anthropogenic contaminants (Blum et al., 2015; Allen, 2018). They have been linked to harmful health effects, including reduced kidney function, metabolic syndrome, thyroid disruption, and adverse pregnancy outcomes (Agency for Toxic Substances and Disease Registry (ATSDR), 2020).

PFAS contain one or more carbon atoms with fluorine in place of hydrogen to form the moiety C_nF_{2n+1}-R, where R represents functional groups (e.g., sulfonate, carboxylic acid) (Blake and Fenton, 2020; Interstate Technology and Regulatory Council (ITRC), 2020). The per- or polyfluoroalkyl moiety is chemically and thermally stable, and it exhibits both lipophilic and hydrophilic properties (Interstate Technology and Regulatory Council (ITRC), 2020), making PFAS ideal as both surfactants and surface protection products. PFAS have been used in grease-resistant papers for food containers/wrappers, stain-resistant coatings on carpets and upholstery in home and vehicle products, water-resistant clothing and footwear, cleaning products, shampoo, dental floss, nail polish and eye makeup, paints, varnishes, ski wax and sealants, and aqueous film-forming foams for civilian and military firefighting (Agency for Toxic Substances and Disease Registry (ATSDR), 2019).

The desirable chemical properties of many PFAS paradoxically impart environmentally and biologically undesirable properties such as environmental and biological persistence. PFAS accumulate in the serum, lungs, kidney, liver, and brain, including fetal organs (Perez et al., 2013; Mamsen et al., 2019; Cao and Ng, 2021). Human exposure to PFAS is associated with adverse effects on the immune (National Toxicology Program (NTP), 2016), endocrine, metabolic, and reproductive systems (including fertility and pregnancy outcomes), and increased risk for cancer (Agency for Toxic Substances and Disease Registry (ATSDR), 2020).

PFAS exposure is considered ubiquitous in the U.S. (CDC, 2019) and around the world, with perfluorooctanoate (PFOA) and perfluorooctane sulfonate (PFOS) detectable in > 90% of representative study populations (Kato et al., 2011; Bjerregaard-Olesen et al., 2017; Ye et al., 2018). Diet and drinking water are the main sources of exposure for adults, though this varies with lifestyle, diet, proximity to point and nonpoint sources, and local drinking water contamination levels. Formula-fed infants are thought to be the most highly exposed members of the human population due to their high water intake to body weight ratio (Goeden, 2018; Goeden et al., 2019). Drinking water may be the largest source of PFAS exposure for communities impacted by high levels of PFAS contamination (Environmental Working Group, 2020).

A handful of PFAS (such as PFOA and PFOS) are extensively studied, but very little is known about the toxicity of the thousands of other PFAS that can occur in the environment (Ankley et al., 2021). To date, many PFAS have not been systematically tested. Traditional one-by-one toxicity testing using laboratory rodents is too expensive, slow, and impractical to evaluate the hazard of the PFAS chemical space (Patlewicz et al., 2019). A more practical way is to identify and prioritize those PFAS with the most potential to cause adverse human health or environmental effects (Ankley et al., 2021). It is critical to assess as many PFAS as possible in a high-throughput manner in the same platform as part of this prioritization effort. A subset of PFAS has been assessed using *in vitro* assays: 17 PFAS were flagged as active in at least one of the battery of US Environmental Protection Agency (US EPA) ToxCast high-throughput assays on their Chemical Dashboard. Another 113 unique structures were evaluated *in vitro* by Houck et al. (Houck et al., 2021). They confirmed expected activities for previously studied PFAS and found novel bioactivities, in particular RXRβ agonism. However, the effects of metabolism on PFAS are quite limited *in vitro*. A whole animal model avoids this limitation, but *in vivo* data remain scarce relative to the diversity of PFAS structures.

The developmental zebrafish platform can be deployed as a sensitive whole animal biosensor of PFAS hazard. Zebrafish can span the scientific gap between *in vitro* and traditional mammalian models (Horzmann and Freeman, 2018). They have rapid, transparent development and share significant genetic homology with humans (Howe et al., 2013; Truong and Tanguay, 2017). Previous PFAS studies in developmental zebrafish found morphological and behavior effects (Ulhaq et al., 2013; Jantzen et al., 2016; Rericha et al., 2021; Wasel et al., 2021), and identified structure driven trends in bioactivity and bioconcentration (Menger et al., 2019, 2020; Vogs et al., 2019; Gaballah et al., 2020). While one study conducted a high content screen of 58 PFAS (Rericha et al., 2021), most have focused on fewer structures. We used the developmental zebrafish to evaluate and compare the toxicity of a 139 structure PFAS library assembled by the US EPA (Patlewicz et al., 2019). The goal was to assess the library for the developmental and neurotoxic potential across 13 morphological endpoints and 2 behavioral assessments. Structure-activity relationships were modeled based on chemotypes, physicochemical properties, and developmental bioactivity. The multi-dimensional zebrafish platform allowed rapid hazard ranking of PFAS chemotypes. Hopefully, these data prioritize further testing that will inform the selection of safer alternatives.

2. Methods: experimental design + analysis

2.1. Chemical library procurement

The library of 139 PFAS was procured from the US EPA Center for Computational Toxicology & Exposure (CCTE) as a subset of the library of 430 (https://comptox.epa.gov/dashboard/chemical_lists/EPAPFASINV). A table of the individual PFAS and CAS numbers is provided (Table S1). Parathion ethyl (CAS 56-38-2) was purchased from Sigma-Aldrich in the PESTANAL analytical standard grade as a positive control for zebrafish developmental toxicity.

2.2. PFAS structure categorization

To align with existing knowledge of the PFAS chemicals, the 139 PFAS were systematically evaluated to determine whether each structure belonged to a previously defined category (Buck et al., 2011; Patlewicz et al., 2019; Kwiatkowski et al., 2020), or via the EPA's CompTox Chemicals Dashboard PFAS Markush Structure-based Categories List (https://comptox.epa.gov/dashboard/chemical_lists/EPAPFASCAT). Existing unique categories were identified from these sources, noting representative chemical structures when available and combining relatively similar categories (e.g., the "polyfluoroalkyl (linear) alcohol" category defined by the Markush list was combined with the more general "polyfluorinated alcohol" of Patlewicz et al. and ultimately termed "perfluoroalkyl alcohol"). Each of the 139 PFAS structures was then evaluated for fit within each available category based on the structural definition (Table S1), creating a natural division into perfluorinated or polyfluorinated categories. PFAS with structures that did not align with previously defined categories (e.g., undefined difunctional or halide structures) were labeled as "other," which included chemicals that are both perfluorinated and polyfluorinated.

2.3. Zebrafish husbandry

Tropical 5D wild-type zebrafish were housed at Oregon State University's Sinnhuber Aquatic Research Laboratory (SARL, Corvallis, OR)

in densities of 1000 fish per 100-gallon tank according to the Institutional Animal Care and Use Committee protocols (Barton et al., 2016). Fish were maintained at 28 °C on a 14:10 h light/dark cycle in recirculating filtered water, supplemented with Instant Ocean salts. Adult, larval and juvenile fish were fed with size-appropriate GEMMA Micro food 2–3 times a day (Skretting). Spawning funnels were placed in the tanks the night prior, and the following morning, embryos were collected and staged (Kimmel et al., 1995; Westerfield, 2007). Embryos were maintained in embryo medium (EM) in an incubator at 28 °C until further processing. EM consisted of 15 mM NaCl, 0.5 mM KCl, 1 mM $MgSO_4$, 0.15 mM KH_2PO_4, 0.05 mM Na_2HPO_4, and 0.7 mM $NaHCO_3$ (Westerfield, 2000).

2.4. PFAS exposures

Embryos were dechorionated at 4 h post-fertilization (hpf) and exposed in 96 well plates as described in (Truong et al., 2014). The standard plate layout consisted of 10 PFA concentrations (0.015, 0.046, 0.14, 0.41, 1.23, 3.7, 11.1, 33.33, 66.5, 100 μM, n = 7) and positive control (parathion ethyl at 19.3, 24.2, 29.1, and 34.0 μM, n = 3) on the same plate (Fig. 1). Parathion is routinely used as a positive control in the lab as it induces reproducible morphological defects. All PFAS chemicals and the parathion ethyl positive control were delivered to the individual wells of a 96-well plates filled with 100 μL of embryo medium, one embryo per well, using an HP D300 digital dispenser from the master stocks (30, 20, 10, or 5 mM) provided by the US EPA dissolved in dimethyl sulfoxide (DMSO), and a 10 mM parathion ethyl stock in DMSO. A complete list of PFAS stocks and concentrations is provided in Table S1. The DMSO concentration in all plate wells was normalized to 0.33% using the D300 dispenser. Test concentrations were selected to maximize the probability of encountering the effective concentration at which 80% of the test population experienced any morphological effect (EC_{80}) while avoiding solubility limits and also ensuring concentrations appropriate to behavior endpoints, all in one experiment. Each plate was tested in duplicate with a total of 10 concentrations (n = 14 embryos per PFAS concentration), 24 solvent control (0.33% DMSO), and 6 per parathion ethyl concentration.

Immediately after chemical addition, plates were sealed with parafilm between the plate and its lid and incubated at 28° ± 1 °C overnight on an orbital shaker at 235 RPM (Truong et al., 2016) until 24 hpf, when embryonic photomotor response (EPR), mortality, and morphology were assessed. Plates were then returned to the dark incubator until 120 hpf when larval photomotor response (LPR), mortality, and morphology were evaluated.

2.5. Developmental toxicity assessments

2.5.1. Mortality and morphology

At 24 hpf, embryos were screened for mortality and 2 developmental endpoints. At 120 hpf, mortality and incidence of abnormality in 9 morphology endpoints were evaluated as binary outcomes (Table S2 for a description of morphological endpoints).

2.5.2. Photomotor responses

The embryonic photomotor response (EPR) assay was conducted at 24 hpf, taking care not to expose the test plates to visible light prior to the assay (Reif et al., 2016). Briefly, EPR images were captured only with infrared light (IR band pass filter at camera), while the photomotor stimulus consisted of two 1 s pulses of white visible light (13 kilolux) at 30 and 40 s after video recording began. The nine seconds prior to the first pulse were considered the "background" (B) period; the nine seconds immediately after the first pulse were considered the "excitatory" (E) period; the nine seconds following the second pulse were considered the "refractory" (R) period. During each period, test embryos may exhibit normal or hypo- or hyper-activity relative to the on-plate control animals, indicating chemical-induced effects on non-visual (eyes are not

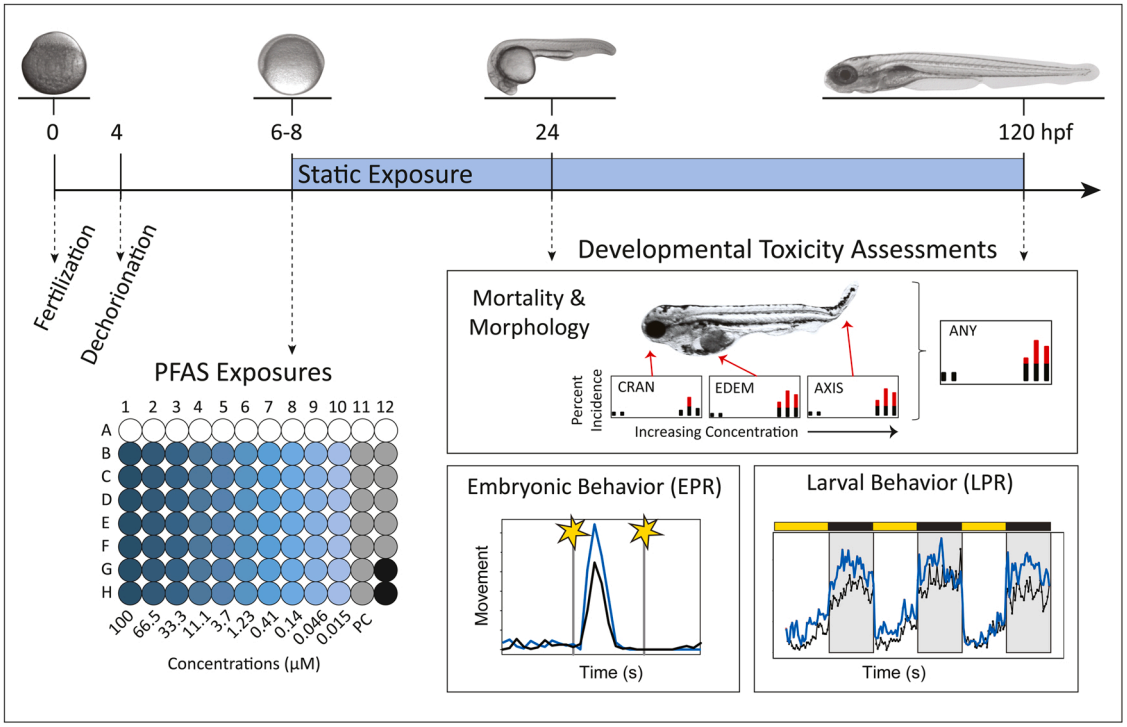

Fig. 1. Overall Experimental Design. Embryonic zebrafish were developmentally exposed from 6 to 120 hpf (top; hpf = hours post-fertilization). The embryos were exposed to 10 concentrations of PFAS (plate design: all shades of blue), 4 concentrations of PC (parathion ethyl positive control; gray), and vehicle control (white). At 24 and 120 hpf, embryos were assessed for mortality and 10 morphological endpoints and a summary endpoint (ANY). Examples are: CRAN = craniofacial malformations, EDEM = edema, AXIS = bent axis. Embryonic and Larval Photomotor Response are behavior assays in which movement was assessed in response to 2 flashes of light or alternating light/dark cycles at 24 and 120 hpf.

functional at 24 hpf) photomotor development (Kokel et al., 2013).

The larval photomotor response (LPR) assay was conducted at 120 hpf when the 96-well plates of larvae were placed into ZebraBox behavioral analysis chambers (Viewpoint Behavior Technology) and larval movement tracked with ZebraLab motion analysis software for 24 min across 4 cycles of 3 min light: 3 min dark. The distance moved by each larva in the 4th light/dark cycle was integrated over 6 s binning periods.

It should be noted that while both the EPR and LPR assays assessed photomotor response, EPR is strictly based on the response of photoreceptors within the hindbrain, prior to eye vision, while LPR is visual. Both responses represent a behavioral effect and the mechanism leading to each effect can differ for a single compound. Additionally, the EPR assay takes place at 24 hpf, potentially before the affected system/tissue is developed enough for the chemical to have the effect(s) observed at 5 dpf; therefore, a response in either assay was considered bioactive independently of the other.

For all assessments, data were collected from embryos exposed to nominal PFAS concentration and were uploaded under a unique well-plate identifier into a custom LIMS (Zebrafish Acquisition and Analysis Program (ZAAP)) – a MySQL database and analyzed using custom R scripts that were executed in the LIMS background (Truong et al., 2016). All data can be found at: https://github.com/Tanguay-Lab/Manuscripts.

2.6. Statistical analysis

2.6.1. Morphology

Following chemical exposure, the incidence of a morphological effect was recorded as binary (0 or 1) response in any of 13 endpoints (Table S2). During analysis, responses across all these endpoints were collapsed into a singular binary (0 or 1) morphology endpoint named 'ANY'. A benchmark dose (BMD) approach was applied to morphologically bioactive samples on the summary statistic of 'ANY' endpoint using a *parametric* curve fitting process. Briefly, this data was modeled using the unrestricted 3-parameter log-logistic model for dichotomous data with "extra risk" and was implemented following guidelines from the EPA BMDS v3.2 manual (US Environmental Protection Agency (EPA), 2020). A benchmark response (BMR) was defined as a 10% change relative to the background response and BMD_{10} values were calculated.

2.6.2. Dose-response modeling of behavior data

For EPR, the recorded periods at the beginning of the experiment (immediately surrounding the initiation/termination of camera recording) were truncated to assure equivalence in recorded experimental period for all chemicals. The statistical analysis of activity considered only the Background (B), Excitatory (E), and Refractory (R) intervals. For LPR, movement data from the 15 frames s^{-1} capture was integrated into 6 s bins and responses from light and dark phases were analyzed independently. A comprehensive analysis of the behavior response patterns was carried out using the BMD methodology with a 10% benchmark response threshold (Thunga et al., 2021). Any dead or malformed animals were removed from behavior analysis, and concentrations in which more than 30% of the individuals were malformed were also removed. A quantitative dose-response analysis of behavior data was performed by fitting a 4-parameter log-logistic model to the response values. Behavior response values were computed as the average movement value over the defined time interval (Background/Excitatory/Refractory for EPR and Light/Dark for LPR). These values were assumed to follow a zero-augmented gamma distribution. Most model fittings were done by maximum likelihood estimation using only non-zero response values. However, if there were concentrations where the number of zero response values was more significant than the number of non-zero response values, then a penalty was added to the likelihood function that favored curve fit values closer to zero and a shallower slope. In both cases, the gamma distribution shape parameter was assumed to be constant and included in the optimization process. Hyperactive curve fitting was done using a subset of concentrations up to the highest dose where the mean response value at that dose was greater than the mean control response, and the response had not decreased more than 20% from the next lower dose. Hypoactive curve fitting used data from all concentrations. Curve fits were required to have the second asymptote outside the band of control mean response + /- 50%. BMD values were computed using the same equation as the morphology endpoints since both data types were fit using log-logistic models. Finally, post-hoc quality control was performed by visually inspecting each of the curve fits and removing any unreliable fits due to high variability among the treated groups or high overlap between the control and treated groups, especially near the BMD value. Only hits that passed this final QC check were reported in the SI table.

2.6.3. Chemical property analysis

Five physicochemical properties were obtained from the US EPA's Chemical Dashboard for the 139 PFAS and assessed for statistical association with bioactivity. The physicochemical properties included for this analysis were the average mass, Opera-predicted octanol-air partition coefficient (Log K_{OA}), Opera-predicted octanol-water partition coefficient (log P), predicted vapor pressure (mm Hg), and the number of fluorinated carbons (manually determined) (Table S1). Association between these properties and bioactivity were only evaluated for PFAS manually classified as volatile (see below). Since these predicted values were predominantly determined using QSARs based on training sets of mostly volatile compounds, there was less accuracy to predict non-volatile PFAS that are largely ionized at environmental pH. A chemical's BMD_{10} values in each of the 3 assays (morphology, EPR, and LPR) were used to measure bioactivity. Since very few chemicals showed bioactivity and the data had several tied ranks, the Kendall rank correlation method was used to test for association.

PFAS volatility was determined by manually curating each chemical's structure, as obtained from the EPA's CompTox Chemicals Dashboard, and sorting it into volatile or non-volatile categories. Chemicals were sorted for volatility based on the structure, such as functional groups and sites that could release and/or accept protons. Those that could be ionized are suitable for analysis by liquid chromatography (non-volatile), while those that are non-ionizable are better suited for gas chromatography (volatile). For those chemicals that did not fall into one of the two categories solely based on structure, a program, Chemicalize, was used to predict volatility. The software used chemical identifiers (i.e., molecule name, registry number, SMILES, or InChI) as input, and predicted pKa and ion speciation. Compounds for which the software could not supply pKa and ion speciation were assigned as volatile.

2.6.4. Chemotype enrichment analysis

Chemical feature enrichments across the PFAS library were explored using ToxPrint chemotypes downloaded from EPA's CompTox Chemicals Dashboard (https://comptox.epa.gov/dashboard/dsstoxdb/batch_search). The large set of publicly available ToxPrint chemotypes collapsed into 36 broader chemotype categories (Table S3). Enrichment analysis for each category was done using contingency tables and Fisher's exact test (p-value <0.05) to check if chemicals that were active in specific assays were enriched for any structural features. Chemotypes present in less than 5% of all chemicals in the dataset were removed from the analysis.

3. Results and discussion

3.1. Commonly studied PFAS - ranked potency to impact zebrafish development

Of the 139 structurally diverse PFAS, 49 (35%) induced either

abnormal morphology, embryonic and larval photomotor response (EPR and LPR, respectively) or a combination as determined by benchmark dose (BMD) analysis (Fig. 2a). In total, 31 PFAS (22%) induced morphological effects, 11 (7%) elicited abnormal embryonic behavior, and 25 (17%) caused abnormal larval behavior (Fig. 2b). The median morphological BMD_{10} for the 31 PFAS was 31.89 μM. The most potent PFAS was perfluorodecanoic acid (PFDA), with the lowest BMD_{10} for morphological effects of 0.223 μM. The least potent was perfluorooctanesulfonyl fluoride (PFOS-F), with a BMD_{10} of 86.05 μM. PFDA was previously evaluated in ToxCast assays and numerous other studies, while PFOS-F, a PFOS precursor (Butenhoff et al., 2017), has very limited toxicity data. Both PFDA and PFOS-F are in the perfluoroalkyl group with different functional groups: carboxylic acid, and sulfonyl fluoride, respectively and with vastly different Log K_{OA} (4.23 vs 3.33, respectively) and LogP (3.13 vs 1.53). Although the Log K_{OA} was dramatically different, these values are estimates from models that do not apply well to anionic chemicals such as carboxylates. Previous studies reported significant toxicity resulting from PFDA exposure (Lau et al., 2004), specifically compared to other shorter-chain perfluoroalkyl carboxylates, in developmental zebrafish (Ulhaq et al., 2013) and other animal models (Olson and Andersen, 1983; Kim et al., 2013). However, many studies reported greater toxicity from the perfluoroalkyl sulfonic acid head group compared to a perfluoroalkyl carboxylic acids (Ulhaq et al., 2013; Menger et al., 2019; Gaballah et al., 2020). Of the 8 PFAS most commonly studied *in vivo*, the potency ranking (based on morphological effects) is: PFDA > perfluorooctanesulfonamide (FOSA) > PFOS > perfluoroheptane sulfonic acid (PFHpS) > perfluorotridecanoic acid (PFTrDA) > 8:2 fluorotelomer sulfonic acid (8:2 FTS) > perfluoroundecanoic acid (PFUndA) > perfluorohexane sulfonic acid (PFHxS) > PFOS-F. All but PFOS-F were non-volatile PFAS, which could be another explanation of the potency ranking where PFOS-F was the least bioactive in this screen.

3.2. Embryonic photomotor behavior was impacted by 11 different PFAS structures

Behavior endpoints affected by PFAS exposures varied based on assay and endpoint. Aberrant embryonic photomotor response (EPR) behavior at 24 hpf was predominately detected during the excitatory phase of the assay. Six compounds induced hyperactivity in this period: perfluorooctanesulfonamide (FOSA); 1H,1H,10H,10H-perfluorodecane-1,10-diol; 3-(perfluoroisopropyl)-2-propenoic acid, perfluorooctyl (ethyl)phosphonic acid, 6:2 fluorotelomer phosphate monoester, and (heptafluorobutanoil)pivaloylmethane). Five induced a hypoactive EPR: 1H,1H,8H,8H-perfluorooctane-1,8-diol; 1H,1H,7H-perfluoroheptyl-4-methylbenzenesulfonate; 1-(perfluorohexyl)octane; 8:2 FTS, and 2H,2H,3H,3H-perfluorooctanoic acid. In Fig. 2a; EPR hyperactivity is displayed in yellow and hypoactivity is displayed in green. The lowest BMD_{10} for the EPR excitatory phase were 1H,1H,10H,10H-perfluorodecane-1,10-diol and 1H,1H,8H,8H-perfluorooctane-1,8-diol, both

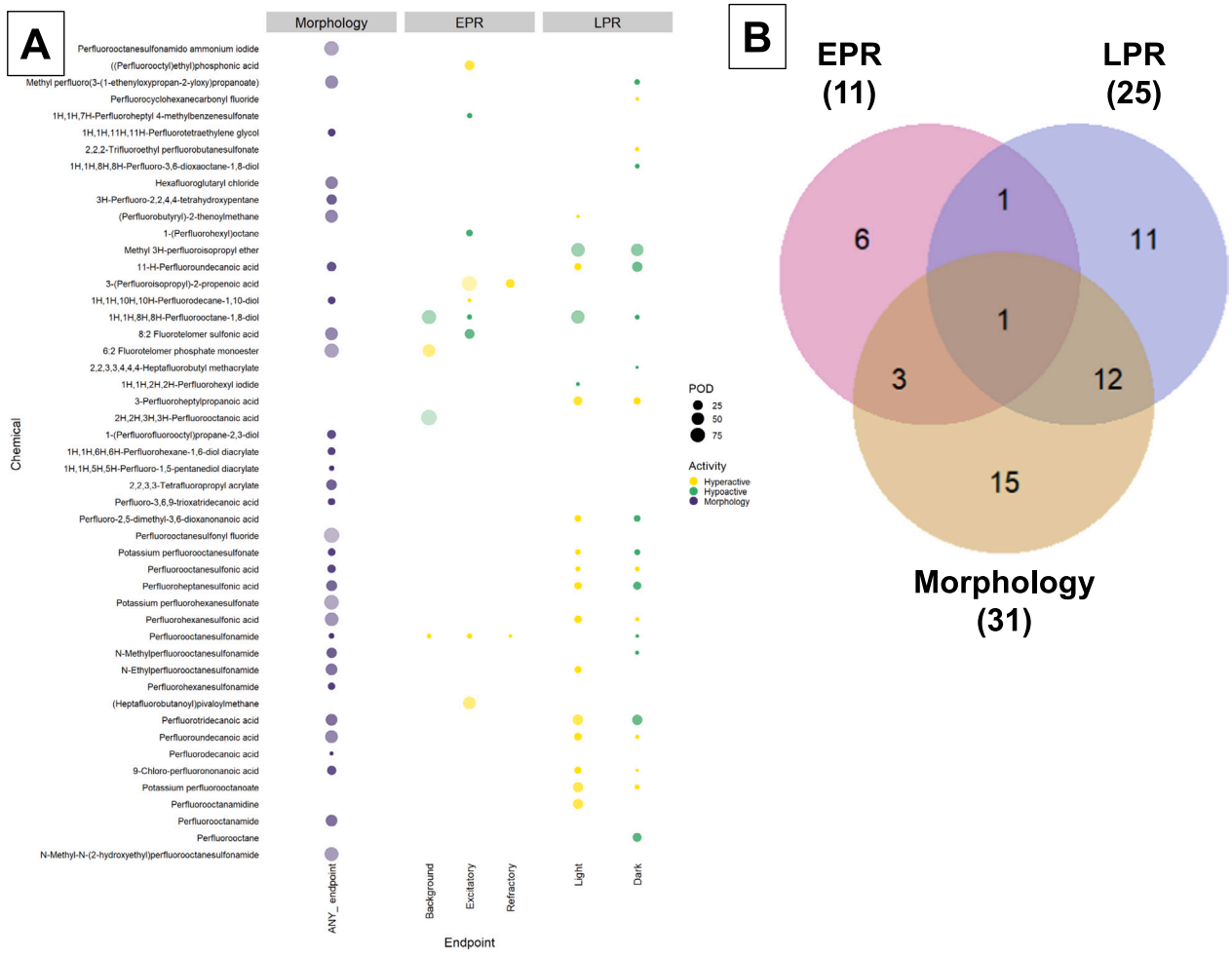

Fig. 2. Developmental toxicity screening using the embryonic zebrafish model. A. Summary of Developmental Toxicity Bioactivity. Dots are colored by their activity (hypo vs hyper), their size represents Point Of Departure (POD) estimate (larger = higher POD), and transparency levels represent the potency (darker = more potent). **B.** Venn Diagram of the number of PFAS that were bioactive in morphology, embryonic photomotor response (EPR), and larval photomotor response (LPR) assays.

fluorotelomer symmetric diols for which there is very limited available toxicity information.

Activity in the refractory phase is abnormal by definition, but 3-(Perfluoroisopropyl)-2-propenoic acid, and FOSA induced refractory phase hyperactivity. These two PFAS were also associated with excitatory phase hyperactivity. The PFAS 6:2 fluorotelomer phosphate monoester was associated with hyperactivity in the EPR background phase, and 2H,2H,3H,3H-perfluorooctanoic acid was associated with hypoactivity in the EPR background phase; neither PFAS was associated with any other EPR effects. The EPR is a rapidly assayable endpoint detected below the threshold for teratogenicity. As such it can define unique patterns of hazard potential and prioritize chemicals that impact early development (Carbaugh et al., 2020) and that likely also impact later development (Reif et al., 2016; Ortmann et al., 2022).

3.3. LPR behavior was impacted by 25 different PFAS structures

Normal zebrafish LPR behavior at 120 hpf is characterized by low, almost baseline activity in the visible light phases and 3–10 fold more swimming g activity in the dark phases. Here 17 and 21 PFAS elicited aberrant behavior in the light and dark phases, respectively. Most PFAS induced hyperactivity in the light period while only 3 compounds induced hypoactivity. The opposite trend was observed for the dark period of the LPR assay where PFAS mostly elicited hypoactivity.

A total of 15 PFAS were bioactive in both the light and dark phases of LPR with BMD values spanning 1000 fold (0.045–52.45 μM). Notably, only FOSA caused abnormalities in EPR, LPR and morphology. FOSA is one of the 17 PFAS evaluated in ToxCast assays. With a hit rate of 16% (125/795 total assay endpoints) it was almost 2x higher than the median hit rate for the ToxCast PFAS (8%). FOSA, an intermediate metabolite of longer-chain PFOS precursors (Martin et al., 2010), has been identified in previous studies as particularly bioactive compared to other PFAS in zebrafish (Dasgupta et al., 2020) and neurotoxic *in vitro* (Slotkin et al., 2008). It is a metabolite of n-ethyl perfluorooctane sulfonamide (EtFOSA), an active ingredient in sulfluramid, a pesticide commonly used to control leaf-cutting ants in equatorial countries such as Brazil. The use of sulfluramid has reportedly led to FOSA detection in environmental samples suggestive of a significant potential for human exposure (Nascimento et al., 2018). One proposed mode of action for FOSA toxicity that could explain its potency in all three assays is disruption of mitochondrial bioenergetics (Starkov and Wallace, 2002), to which the embryonic zebrafish model is particularly sensitive (Fichi et al., 2019).

Assessments revealed that over a third (35%) of PFAS within a diverse library exhibited bioactivity manifest as both malformations and altered behavior in developing zebrafish. The diversity of endpoints affected across similar chemical concentrations suggested that modes of action likely differed between structure groups and that the 49 bioactive PFAS have the potential to adversely impact human health. These PFAS and their closely related structures in the PFAS universe outside this library should be prioritized for definitive hazard characterization. Detailed structure-activity modeling can reveal the features that drive their toxicity and inform the field on PFAS structures to avoid.

3.4. Low PFAS volatility drives developmental toxicity

The volatility of a chemical could influence its bioactivity under a given set of test conditions. PFAS were sorted into volatile and non-volatile categories via a decision tree with manual curation. The 139 member library consisted of largely volatile PFAS (59%). Among the 31 PFAS that induced morphological effects, 12 (39%) were categorized as volatile and 19 (61%) as non-volatile (Fig. 3). The majority of the non-active PFAS in any of the assays were volatile, suggesting that PFAS volatility was a driver of bioactivity under the test conditions used. A Fisher's exact test of counts of the number of volatile and non-volatile PFAS detected in each assay showed that volatile PFAS were likely to be flagged as inactive by LPR and morphology endpoints (p-value <0.05). Higher volatility would lessen the amount of PFAS available to interact with the embryo. This trend was not observed in the earlier EPR assay where 5 out of the 11 bioactive compounds were volatile (45%). Volatility might have resulted in lower bioavailability that precluded LPR and morphology effects but was sufficient to impact early behavior, perhaps only transiently. Overall, the present study identified an association between volatility of PFAS and its bioactivity in the developing zebrafish.

3.5. Limited correlation between 5 physicochemical properties and PFAS toxicity

Average mass, number of fluorinated carbons, LogP, Log K_{OA}, and vapor pressure were compared to PFAS bioactivity. The median average mass of the 139 PFAS was 380 g/mole. The individual PFAS average masses ranged from 163 to 726 g/mole; all were generally considered low molecular weight PFAS, as opposed to high molecular weight fluoropolymers (Buck et al., 2011). Average mass did not significantly correlate with chemical toxicity when considering morphological

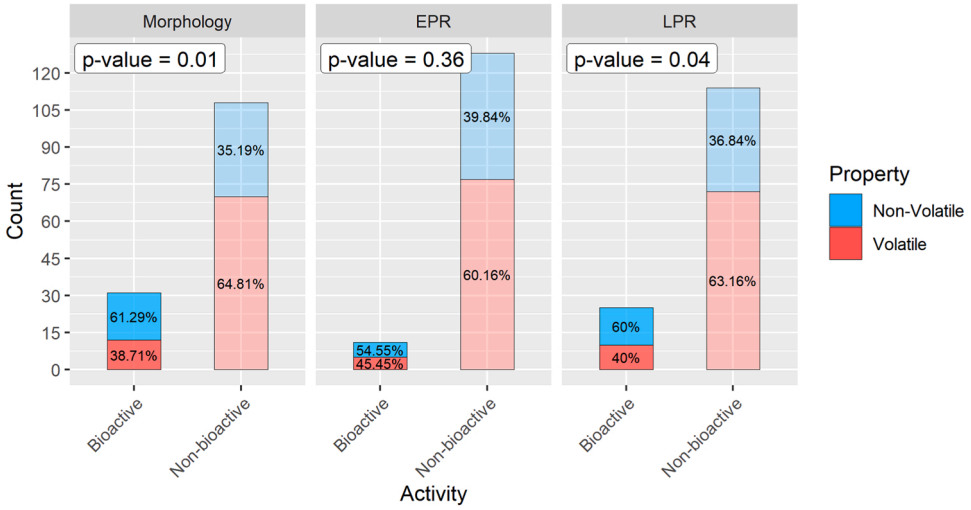

Fig. 3. Bar plot showing break -down of chemicals' bioactivity and volatility across each endpoint tested. Red shaded regions represent the number of volatile compounds in that category and blue shaded regions represent the number of non-volatile compounds in that category. A Fisher's exact test was applied to the counts of the number of volatile and non-volatile PFAS detected in each assay ($p < 0.05$).

bioactivity (R = 0.24; p = 0.31), EPR (R = −0.4; p = 0.48), or LPR (R = 0.29; p = 0.29) assays in the present study (Fig. S1). Within a comparable mass range, a recent *in vitro* study by Houck et al. found a lower incidence of bioactivity for lower molecular weight PFAS, but cautioned that their results may have been skewed by false negatives due to poor analytical quality control and volatilization (Houck et al., 2021). Few toxicological studies have distinguished between PFAS in this mass range by molecular weight. PFAS are differentiated by fluorinated alkyl chain length. PFAS chain lengths are typically applied to the most commonly studied perfluoroalkyl carboxylic acids and sulfonic acids. Note that fully-fluorinated carbons were not representative of the broader structural diversity in this library of polyfluorinated substances. A more suitable criterion was simply the number of fluorinated carbons.

The number of fluorinated carbons per chemical ranged from 2 to 13 with 6 being the median (20 chemicals). Correlation analysis bioactive PFAS versus number of fluorinated carbons for morphology (R = 0.17; p = 0.47) and LPR (R = 0.34, p = 0.19) indicated no correlation, but there was a statistically significant inverse correlation for EPR (R = −0.84, p = 0.05) where increased number of fluorinated carbons resulted in lower BMD_{10} values. Previous studies found that PFAS toxicity (and bioaccumulation) increased with increasing alkyl chain length (Gaballah et al., 2020; Ankley et al., 2021). The correlation with EPR, but not morphology or LPR suggested that, at least among a diverse library, number of fluorinated carbons alone does not explain variation in toxicity in larval zebrafish.

The PFAS library had a median LogP of 3.5, and no significant correlation was found between PFAS morphology outcomes and LogP (R = −0.03; p = 0.95), EPR (R = 0.4; p = 0.48), or LPR (R = −0.24; p = 0.38). Likewise no correlation was found between PFAS morphology outcomes and Log K_{OA} (R = −0.27; p = 0.25), or LPR (R = −0.29; p = 0.29), but a statistical correlation was observed for EPR (R = −1; p = 0.02). The higher the Log K_{OA}, the lower the BMD_{10} values were. The PFAS library median vapor pressure was 0.54 mm Hg. No correlation was found between EPR, LPR or morphology outcomes and PFAS vapor pressure (EPR R = 0; p = 1; LPR R = 0.29; p = 0.29; morphology R = 0.12; p = 0.64). In summary, there was no correlation between the 5 physiochemical properties and PFAS bioactivity at 120 hpf, but number of fluorinated carbons and the Log K_{OA} had an inverse relationship with EPR BMD_{10} at 24 hpf. The photomotor excitation detected in EPR is dependent on hindbrain photoreceptors, but different mechanisms may control the response (Kokel et al., 2013). Therefore, the correlation observed in this assay suggested that two physicochemical properties – increasing fluorinated carbon chain length and the corresponding increase in Log K_{OA} - can perturb, at least transiently, nonvisual photomotor behavior. While 2 H, 2 H,3 H,3 H-perfluorooctanoic acid was associated with hypoactivity in the baseline phase of the EPR we did not directly assay for the baseline (unstimulated, spontaneous) tail bending by monitoring 24 hpf embryos for more than 30 s. This may not have been not long enough to obtain a robust baseline of spontaneous frequency, typically once every 15 s or so at 28 °C. Spontaneous tail bending is vitally important to muscle development needed to break out of the chorion around 48 hpf. Further study of chorion-intact embryos exposed to longer chain PFAS, while monitoring tail flexions, may shed light on whether some PFAS depress motor activity and hatch fitness.

3.6. PFAS structural categories did not generally predict bioactivity

Structure-activity modeling used the PFAS landscape defined by the US EPA's CompTox Chemicals Dashboard Markush Categories list and several other studies (Buck et al., 2011; Patlewicz et al., 2019; Kwiatkowski et al., 2020). The 139 PFAS represented 30 structural categories, of which 13 categories were perfluorinated compounds (56 PFAS) and 16 of categories were polyfluorinated compounds (51 PFAS) (Fig. 4). Among these 107 chemicals, there was no significant enrichment of bioactivity in either the per- or polyfluroniated category (p = 0.42). A total of 32 PFAS structures (23%) did not fall into previously defined categories, and were classified "other," including perfluorinated and polyfluorinated PFAS. However there were more than twice as many bioactive PFAS in the "other" category than in any of the CompTox-Markush categories. Improved definition of these categories is needed.

Forty-nine PFAS representing 20 of the 29 structural categories were identified as bioactive in at least one assay, spanning both the perfluorinated (15), polyfluorinated (16), and other domains. A significant portion of the perfluoroalkyl carboxylic acids, perfluoroalkyl sulfonamides, perfluoroalkyl sulfonic acids, fluorotelomer acrylates, fluorotelomer carboxylic acids, fluorotelomer symmetric diols, and polyfluoroalkyl carboxylic acids elicited toxicity. But, depending on representation, these categories could also contain an equal or greater number of non-bioactive PFAS, e.g., identity as a perfluoroalkyl

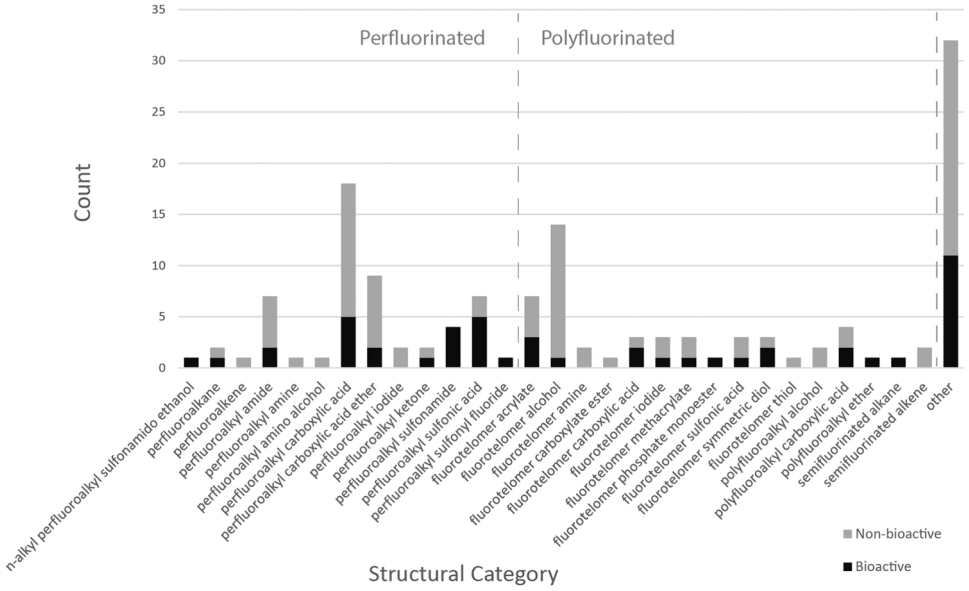

Fig. 4. Bar plot showing breakdown of PFAS into structural categories. Within each bar, the black shaded regions represent the number of PFAS that induced at least one hit in any of the assays and gray represents the number that were not a hit. The gray dotted line in the center of the bar plot divides the PFAS into perfluorinated (left) and polyfluorinated (right, except for the other category).

sulfonamide or sulfonic acid appeared to be quite predictive of bioactivity while identity as a much more highly represented perfluoroalkyl carboxylate was a poor predictor of bioactivity. Low representation in some categories and many bioactives in the "other" category were problematic for a PFAS structure-activity assessment (Cousins et al., 2020). Large size, high diversity and balance should be a goal of future PFAS library screening.

3.7. Generic chemotypes were not more informative than Markush categories

In an attempt to overcome the Markush limitations with this particular library, the effect of recent ToxPrint Chemotype categories was investigated. Chemotypes (CT) are structural fragments that can encode physicochemical, atomic, and electronic properties and are organized by atom, bond, chain, ring types as well as chemical groups including amino acids and carbohydrates. There were 729 essential chemotypes in the current ToxPrint_v2.0 (downloaded from https://toxprint.org/). For the purpose of this analysis, the granular CT landscape was collapsed into 36 supergroups (Fig. 5). In total, 6 supergroup chemtoypes were associated with PFAS developmental toxicity. The proportion of PFAS with the sulfonyl (SO) CT (Table S5) that induced aberrant morphology was statistically higher than the proportion that did not. This was also true for the sulfenamide (SN) and sulfonamide (SON) chemotypes, and alkyl hydroxide (OZ_oxide, acid oxide) in the morphology assays. For behavioral endpoints, the proportion of compounds having the chain.alkaneLinear or OZ_oxide CT resulted in fewer EPR actives, while the SO CT was not correlated with aberrant LPR. Significant correlates emerged from the chemotype analysis, providing promising insight about the utility of predictive toxicology for PFAS. The adoption of chemotypes specific to all of the PFAS landscape should greatly improve the utility of ToxPrint Chemotypes and the present data set. Such a CT set is forthcoming from the US EPA, though a release date has not been published (Richard et al., 2021). The current set of 729 CTs are quite generic, thus CTs that emerged as important here offered little structure-activity insights beyond the previous Markush categories, just statistical significance.

4. Conclusion

The findings suggest that average mass, number of fluorinated carbons, Log P, Log K_{OA}, vapor pressure, and functional head group were generally not predictive of developmental hazard, though Log K_{OA} and number of fluorinated carbons, both closely correlated with each other, together were correlated with aberrant embryo photomotor behavior (inversely correlated with EPR BMD_{10}). Volatility and 6 chemotype structural features were significant correlates with PFAS bioactivity. The effect of volatility might be specific to the experimental system, i.e., zebrafish embryos and larvae in a small volume, static bath exposure, assumed nominal concentration and elevated temperature; a system not directly analogous to traditional toxicology scenarios. Having the ability to rapidly assess the developmental bioactivity *in vivo* has positioned the field to capitalize on forthcoming PFAS-specific chemotypes to understand their structure-activity. PFAS-specific chemotypes could be used to balance a single large library or form multiple smaller targeted libraries. Either approach will present a superior picture of which structural features are hazard liabilities and identify how to select safer alternatives.

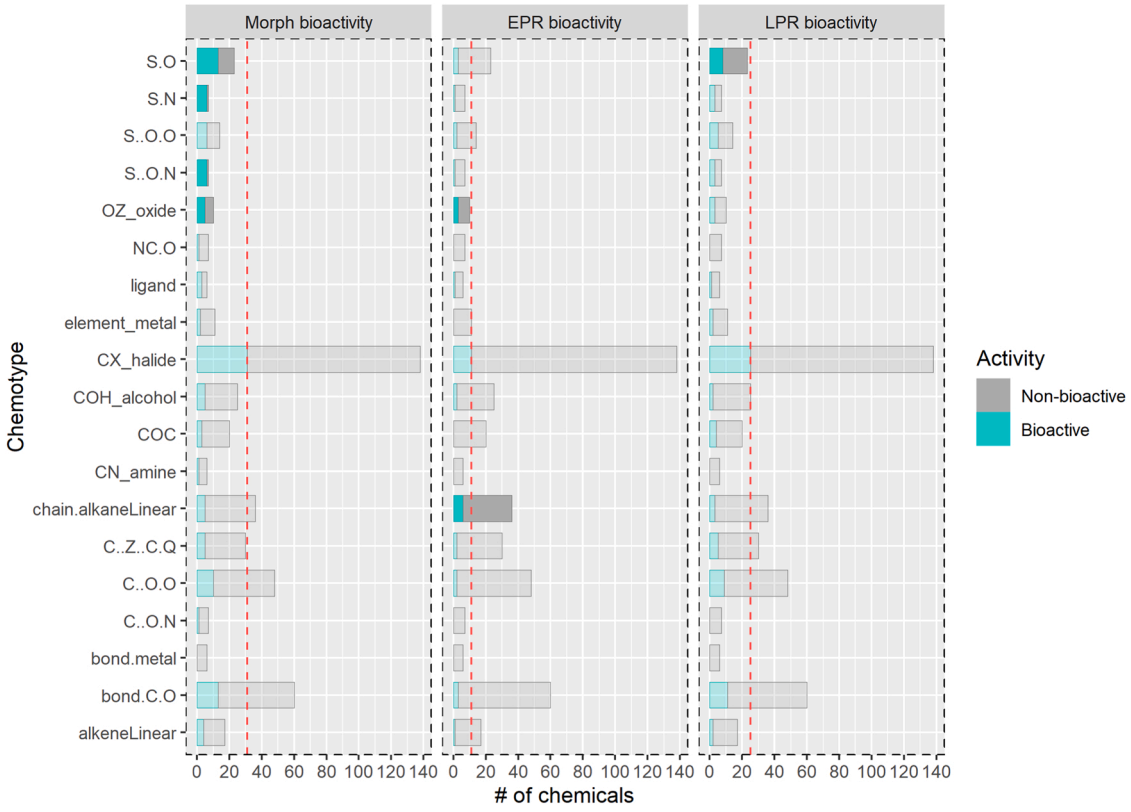

Fig. 5. The vertical axis represents 19 broad chemotype-categories obtained by collapsing Toxprint chemotype into 36 super chemotypes. The horizontal axis represents the number of compounds carrying that chemotype. Each rectangular section represents bioactivity in the indicated assay (Morphology, EPR and LPR). Teal fill represents the compounds that carried a certain chemotype and induced bioactivity in a specific, whereas grey indicates compounds that did not induce bioactivity but carried that chemotype. Chemotypes that were statistically enriched (Fisher Exact Test p-value <0.05) among bioactives or non-bioactives are shown in darker shades. The vertical red dotted line indicates the total number of compounds that induced bioactivity within each assay.

Funding

This research was supported by the National Institute of Environmental and Health Sciences at the National Institutes of Health [P30 ES030287; T32ES007060] and the Environmental Protection Agency [83948101].

CRediT authorship contribution statement

Lisa Truong: Conceptualization, Methodology, Investigation, Data curation, Writing – original draft. **Yvonne Rericha**: Conceptualization, Methodology, Data curation, Writing – original draft. **Preethi Thunga**: Formal analysis, Visualization, Software. **Skylar Marvel**: Formal analysis, Software. **Dylan Wallis**: Formal analysis, Visualization. **Michael Simonich**: Writing – review & editing, Investigation. **Jennifer Field**: Formal analysis. **Dunping Cao**: Formal analysis. **David Reif**: Supervision. **Robyn Tanguay**: Conceptualization, Funding acquisition.

Declaration of Competing Interest

The authors declare that they have no known competing financial interests or personal relationships that could have appeared to influence the work reported in this paper.

Acknowledgment

The authors would like to thank the staff at Sinnhuber Aquatic Research Laboratory for the husbandry care and helping to screen the 139 PFAS in the developmental zebrafish model. Also, our thanks to the US EPA for their generosity in providing the PFAS library.

Appendix A. Supporting information

Supplementary data associated with this article can be found in the online version at doi:10.1016/j.jhazmat.2022.128615.

References

Agency For Toxic Substances And Disease Registry (ATSDR), 2019. PFAS exposure assessments. ⟨https://www.atsdr.cdc.gov/pfas/PFAS-Exposure-Assessments.html⟩. (Accessed April 15 2021).

Agency for Toxic Substances and Disease Registry (ATSDR), 2020. Per- and polyfluoroalkyl substances (PFAS) and your health. ⟨https://www.atsdr.cdc.gov/pfas/health-effects.html⟩. (Accessed April 14 2021).

Allen, J.G., 2018. These toxic chemicals are everywhere - even in your body. And they won't ever go away, The Washington Post.

Ankley, G.T., Cureton, P., Hoke, R.A., Houde, M., Kumar, A., Kurias, J., Lanno, R., McCarthy, C., Newsted, J., Salice, C.J., Sample, B.E., Sepulveda, M.S., Steevens, J., Valsecchi, S., 2021. Assessing the ecological risks of per- and polyfluoroalkyl substances: current state-of-the science and a proposed path forward. Environ. Toxicol. Chem. 40 (3), 564–605. https://doi.org/10.1002/etc.4869.

Barton, C.L., Johnson, E.W., Tanguay, R.L., 2016. Facility design and health management program at the sinnhuber aquatic research laboratory. Zebrafish 13 (Suppl 1), S39–S43. https://doi.org/10.1089/zeb.2015.1232.

Bjerregaard-Olesen, C., Bossi, R., Liew, Z., Long, M., Bech, B.H., Olsen, J., Henriksen, T. B., Berg, V., Nost, T.H., Zhang, J.J., Odland, J.O., Bonefeld-Jorgensen, E.C., 2017. Maternal serum concentrations of perfluoroalkyl acids in five international birth cohorts. Int. J. Hyg. Environ. Health 220 (2 Pt A), 86–93. https://doi.org/10.1016/j.ijheh.2016.12.005.

Blake, B.E., Fenton, S.E., 2020. Early life exposure to per- and polyfluoroalkyl substances (PFAS) and latent health outcomes: a review including the placenta as a target tissue and possible driver of peri- and postnatal effects. Toxicology 443, 152565. https://doi.org/10.1016/j.tox.2020.152565.

Blum, A., Balan, S.A., Scheringer, M., Trier, X., Goldenman, G., Cousins, I.T., Diamond, M., Fletcher, T., Higgins, C., Lindeman, A.E., Peaslee, G., de Voogt, P., Wang, Z., Weber, R., 2015. The Madrid statement on poly- and perfluoroalkyl substances (PFASs). Environ. Health Perspect. 123 (5), A107–A111. https://doi.org/10.1289/ehp.1509934.

Buck, R.C., Franklin, J., Berger, U., Conder, J.M., Cousins, I.T., de Voogt, P., Jensen, A.A., Kannan, K., Mabury, S.A., van Leeuwen, S.P., 2011. Perfluoroalkyl and polyfluoroalkyl substances in the environment: terminology, classification, and origins. Integr. Environ. Assess. Manag 7 (4), 513–541. https://doi.org/10.1002/ieam.258.

Butenhoff, J.L., Olsen, G.W., Chang, S., 2017. Toxicological response of Sprague Dawley rats from inhalation exposure to perfluorooctane sulfonyl fluoride (POSF). Toxicol. Lett. 271, 38–49. https://doi.org/10.1016/j.toxlet.2017.02.017.

Cao, Y., Ng, C., 2021. Absorption, distribution, and toxicity of per- and polyfluoroalkyl substances (PFAS) in the brain: a review. Environ. Sci. Process Impacts 23 (11), 1623–1640. https://doi.org/10.1039/d1em00228g.

Carbaugh, C.M., Widder, M.W., Phillips, C.S., Jackson, D.A., DiVito, V.T., van der Schalie, W.H., Glover, K.P., 2020. Assessment of zebrafish embryo photomotor response sensitivity and phase-specific patterns following acute- and long-duration exposure to neurotoxic chemicals and chemical weapon precursors. J. Appl. Toxicol. 40 (9), 1272–1283. https://doi.org/10.1002/jat.3984.

CDC, 2019. Fourth National Report on Human Exposure to Environmental Chemicals, Updated Tables, January 2019. U.S. Centers for Disease Control and Prevention.

Cousins, I.T., DeWitt, J.C., Gluge, J., Goldenman, G., Herzke, D., Lohmann, R., Miller, M., Ng, C.A., Scheringer, M., Vierke, L., Wang, Z., 2020. Strategies for grouping per- and polyfluoroalkyl substances (PFAS) to protect human and environmental health. Environ. Sci. Process Impacts 22 (7), 1444–1460. https://doi.org/10.1039/d0em00147c.

Dasgupta, S., Reddam, A., Liu, Z., Liu, J., Volz, D.C., 2020. High-content screening in zebrafish identifies perfluorooctanesulfonamide as a potent developmental toxicant. Environ. Pollut. 256, 113550 https://doi.org/10.1016/j.envpol.2019.113550.

Environmental Working Group, 2020. PFAS contamination of drinking water far more prevalent than previously reported. (Accessed November 21 2021).

Fichi, G., Naef, V., Barca, A., Longo, G., Fronte, B., Verri, T., Santorelli, F.M., Marchese, M., Petruzzella, V., 2019. Fishing in the cell powerhouse: zebrafish as a tool for exploration of mitochondrial defects affecting the nervous system. Int. J. Mol. Sci. 20 (10) https://doi.org/10.3390/ijms20102409.

Gaballah, S., Swank, A., Sobus, J.R., Howey, X.M., Schmid, J., Catron, T., McCord, J., Hines, E., Strynar, M., Tal, T., 2020. Evaluation of developmental toxicity, developmental neurotoxicity, and tissue dose in zebrafish exposed to GenX and oher PFAS. Environ. Health Perspect. 128 (4), 47005. https://doi.org/10.1289/EHP5843.

Goeden, H., 2018. Focus on chronic exposure for deriving drinking water guidance underestimates potential risk to infants. Int. J. Environ. Res. Public Health 15 (3). https://doi.org/10.3390/ijerph15030512.

Goeden, H.M., Greene, C.W., Jacobus, J.A., 2019. A transgenerational toxicokinetic model and its use in derivation of Minnesota PFOA water guidance. J. Expo. Sci. Environ. Epidemiol. 29 (2), 183–195. https://doi.org/10.1038/s41370-018-0110-5.

Horzmann, K.A., Freeman, J.L., 2018. Making waves: new developments in toxicology with the zebrafish. Toxicol. Sci. 163 (1), 5–12. https://doi.org/10.1093/toxsci/kfy044.

Houck, K.A., Patlewicz, G., Richard, A.M., Williams, A.J., Shobair, M.A., Smeltz, M., Clifton, M.S., Wetmore, B., Medvedev, A., Makarov, S., 2021. Bioactivity profiling of per- and polyfluoroalkyl substances (PFAS) identifies potential toxicity pathways related to molecular structure. Toxicology 457, 152789. https://doi.org/10.1016/j.tox.2021.152789.

Howe, K., Clark, M.D., Torroja, C.F., Torrance, J., Berthelot, C., Muffato, M., Collins, J.E., Humphray, S., McLaren, K., Matthews, L., McLaren, S., Sealy, I., Caccamo, M., Churcher, C., Scott, C., Barrett, J.C., Koch, R., Rauch, G.J., White, S., Chow, W., Kilian, B., Quintais, L.T., Guerra-Assuncao, J.A., Zhou, Y., Gu, Y., Yen, J., Vogel, J.H., Eyre, T., Redmond, S., Banerjee, R., Chi, J.X., Fu, B.Y., Langley, E., Maguire, S.F., Laird, G.K., Lloyd, D., Kenyon, E., Donaldson, S., Sehra, H., Almeida-King, J., Loveland, J., Trevanion, S., Jones, M., Quail, M., Willey, D., Hunt, A., Burton, J., Sims, S., McLay, K., Plumb, B., Davis, J., Clee, C., Oliver, K., Clark, R., Riddle, C., Eliott, D., Threadgold, G., Harden, G., Ware, D., Mortimer, B., Kerry, G., Heath, P., Phillimore, B., Tracey, A., Corby, N., Dunn, M., Johnson, C., Wood, J., Clark, S., Pelan, S., Griffiths, G., Smith, M., Glithero, R., Howden, P., Barker, N., Stevens, C., Harley, J., Holt, K., Panagiotidis, G., Lovell, J., Beasley, H., Henderson, C., Gordon, D., Auger, K., Wright, D., Collins, J., Raisen, C., Dyer, L., Leung, K., Robertson, L., Ambridge, K., Leongamornlert, D., McGuire, S., Gilderthorp, R., Griffiths, C., Manthravadi, D., Nichol, S., Barker, G., Whitehead, S., Kay, M., Brown, J., Murnane, C., Gray, E., Humphries, M., Sycamore, N., Barker, D., Saunders, D., Wallis, J., Babbage, A., Hammond, S., Mashreghi-Mohammadi, M., Barr, L., Martin, S., Wray, P., Ellington, A., Matthews, N., Ellwood, M., Woodmansey, R., Clark, G., Cooper, J., Tromans, A., Grafham, D., Skuce, C., Pandian, R., Andrews, R., Harrison, E., Kimberley, A., Garnett, J., Fosker, N., Hall, R., Garner, P., Kelly, D., Bird, C., Palmer, S., Gehring, I., Berger, A., Dooley, C. M., Ersan-Urun, Z., Eser, C., Geiger, H., Geisler, M., Karotki, L., Kirn, A., Konantz, J., Konantz, M., Oberlander, M., Rudolph-Geiger, S., Teucke, M., Osoegawa, K., Zhu, B. L., Rapp, A., Widaa, S., Langford, C., Yang, F.T., Carter, N.P., Harrow, J., Ning, Z.M., Herrero, J., Searle, S.M.J., Enright, A., Geisler, R., Plasterk, R.H.A., Lee, C., Westerfield, M., de Jong, P.J., Zon, L.I., Postlethwait, J.H., Nusslein-Volhard, C., Hubbard, T.J.P., Roest Crollius, H., Rogers, J., Stemple, D.L., 2013. The zebrafish reference genome sequence and its relationship to the human genome. Nature 496 (7446), 498–503. https://doi.org/10.1038/nature12111.

Interstate Technology and Regulatory Council (ITRC), 2020. Naming conventions and physical and chemical properties of per- and polyfluoroalkyl substances (pfas). ⟨https://pfas-1.itrcweb.org/fact-sheets/⟩. (Accessed April 15, 2021).

Jantzen, C.E., Annunziato, K.A., Bugel, S.M., Cooper, K.R., 2016. PFOS, PFNA, and PFOA sub-lethal exposure to embryonic zebrafish have different toxicity profiles in terms of morphometrics, behavior and gene expression. Aquat. Toxicol. 175, 160–170. https://doi.org/10.1016/j.aquatox.2016.03.026.

Kato, K., Wong, L.Y., Jia, L.T., Kuklenyik, Z., Calafat, A.M., 2011. Trends in exposure to polyfluoroalkyl chemicals in the U.S. Population: 1999-2008. Environ. Sci. Technol. 45 (19), 8037–8045. https://doi.org/10.1021/es1043613.

Kim, M., Son, J., Park, M.S., Ji, Y., Chae, S., Jun, C., Bae, J.S., Kwon, T.K., Choo, Y.S., Yoon, H., Yoon, D., Ryoo, J., Kim, S.H., Park, M.J., Lee, H.S., 2013. In vivo

evaluation and comparison of developmental toxicity and teratogenicity of perfluoroalkyl compounds using Xenopus embryos. Chemosphere 93 (6), 1153–1160. https://doi.org/10.1016/j.chemosphere.2013.06.053.
Kimmel, C.B., Ballard, W.W., Kimmel, S.R., Ullmann, B., Schilling, T.F., 1995. Stages of embryonic development of the zebrafish. Dev. Dyn. 203 (3), 253–310. https://doi.org/10.1002/aja.1002030302.
Kokel, D., Dunn, T.W., Ahrens, M.B., Alshut, R., Cheung, C.Y., Saint-Amant, L., Bruni, G., Mateus, R., van Ham, T.J., Shiraki, T., Fukada, Y., Kojima, D., Yeh, J.R., Mikut, R., von Lintig, J., Engert, F., Peterson, R.T., 2013. Identification of nonvisual photomotor response cells in the vertebrate hindbrain. J. Neurosci. 33 (9), 3834–3843. https://doi.org/10.1523/JNEUROSCI.3689-12.2013.
Kwiatkowski, C.F., Andrews, D.Q., Birnbaum, L.S., Bruton, T.A., DeWitt, J.C., Knappe, D. R.U., Maffini, M.V., Miller, M.F., Pelch, K.E., Reade, A., Soehl, A., Trier, X., Venier, M., Wagner, C.C., Wang, Z., Blum, A., 2020. Scientific basis for managing PFAS as a chemical class. Environ. Sci. Technol. Lett. 7 (8), 532–543. https://doi.org/10.1021/acs.estlett.0c00255.
Lau, C., Butenhoff, J.L., Rogers, J.M., 2004. The developmental toxicity of perfluoroalkyl acids and their derivatives. Toxicol. Appl. Pharm. 198 (2), 231–241. https://doi.org/10.1016/j.taap.2003.11.031.
Mamsen, L.S., Bjorvang, R.D., Mucs, D., Vinnars, M.T., Papadogiannakis, N., Lindh, C.H., Andersen, C.Y., Damdimopoulou, P., 2019. Concentrations of perfluoroalkyl substances (PFASs) in human embryonic and fetal organs from first, second, and third trimester pregnancies. Environ. Int 124, 482–492. https://doi.org/10.1016/j.envint.2019.01.010.
Martin, J.W., Asher, B.J., Beesoon, S., Benskin, J.P., Ross, M.S., 2010. PFOS or PreFOS? Are perfluorooctane sulfonate precursors (PreFOS) important determinants of human and environmental perfluorooctane sulfonate (PFOS) exposure? J. Environ. Monit. 12 (11), 1979–2004. https://doi.org/10.1039/c0em00295j.
Menger, F., Pohl, J., Ahrens, L., Carlsson, G., Orn, S., 2019. Behavioural effects and bioconcentration of per- and polyfluoroalkyl substances (PFASs) in zebrafish (Danio rerio) embryos. Chemosphere 245, 125573. https://doi.org/10.1016/j.chemosphere.2019.125573.
Menger, F., Pohl, J., Ahrens, L., Carlsson, G., Orn, S., 2020. Behavioural effects and bioconcentration of per- and polyfluoroalkyl substances (PFASs) in zebrafish (Danio rerio) embryos. Chemosphere 245, 125573. https://doi.org/10.1016/j.chemosphere.2019.125573.
Nascimento, R.A., Nunoo, D.B.O., Bizkarguenaga, E., Schultes, L., Zabaleta, I., Benskin, J. P., Spano, S., Leonel, J., 2018. Sulfluramid use in Brazilian agriculture: a source of per- and polyfluoroalkyl substances (PFASs) to the environment. Environ. Pollut. 242 (Pt B), 1436–1443. https://doi.org/10.1016/j.envpol.2018.07.122.
National Toxicology Program (NTP), 2016. National toxicology program monograph on immunotoxicity associated with exposures to pfoa and pfos. ⟨https://ntp.niehs.nih.gov/ntp/ohat/pfoa_pfos/pfoa_pfosmonograph_508.pdf⟩. (Accessed April 15, 2021).
Olson, C.T., Andersen, M.E., 1983. The acute toxicity of perfluorooctanoic and perfluorodecanoic acids in male rats and effects on tissue fatty acids. Toxicol. Appl. Pharm. 70 (3), 362–372. https://doi.org/10.1016/0041-008x(83)90154-0.
Ortmann, J., Altenburger, R., Scholz, S., Luckenbach, T., 2022. Photomotor response data analysis approach to assess chemical neurotoxicity with the zebrafish embryo. ALTEX 39 (1), 82–94. https://doi.org/10.14573/altex.2004021.
Patlewicz, G., Richard, A.M., Williams, A.J., Grulke, C.M., Sams, R., Lambert, J., Noyes, P.D., DeVito, M.J., Hines, R.N., Strynar, M., Guiseppi-Elie, A., Thomas, R.S., 2019. A chemical category-based prioritization approach for selecting 75 per- and polyfluoroalkyl substances (PFAS) for tiered toxicity and toxicokinetic testing. Environ. Health Perspect. 127 (1), 14501. https://doi.org/10.1289/EHP4555.
Perez, F., Nadal, M., Navarro-Ortega, A., Fabrega, F., Domingo, J.L., Barcelo, D., Farre, M., 2013. Accumulation of perfluoroalkyl substances in human tissues. Environ. Int. 59, 354–362. https://doi.org/10.1016/j.envint.2013.06.004.
Reif, D.M., Truong, L., Mandrell, D., Marvel, S., Zhang, G., Tanguay, R.L., 2016. High-throughput characterization of chemical-associated embryonic behavioral changes predicts teratogenic outcomes. Arch. Toxicol. 90 (6), 1459–1470. https://doi.org/10.1007/s00204-015-1554-1.
Rericha, Y., Cao, D., Truong, L., Simonich, M., Field, J.A., Tanguay, R.L., 2021. Behavior effects of structurally diverse per- and polyfluoroalkyl substances in zebrafish. Chem. Res. Toxicol. 34 (6), 1409–1416. https://doi.org/10.1021/acs.chemrestox.1c00101.
Richard, A., Lougee, R., Patlewicz, G., Grulke, C., Williams, A., Yang, C., Rathman, J., Magdziarz, T., 2021. New public CSRML-based structure-fingerprint method for profiling and categorizing PFAS structures for modeling and read-across.
Slotkin, T.A., MacKillop, E.A., Melnick, R.L., Thayer, K.A., Seidler, F.J., 2008. Developmental neurotoxicity of perfluorinated chemicals modeled in vitro. Environ. Health Perspect. 116 (6), 716–722. https://doi.org/10.1289/ehp.11253.
Starkov, A.A., Wallace, K.B., 2002. Structural determinants of fluorochemical-induced mitochondrial dysfunction. Toxicol. Sci. 66 (2), 244–252. https://doi.org/10.1093/toxsci/66.2.244.
Thunga, P., Truong, L., Tanguay, R., Reif, D., 2021. Concurrent evaluation of mortality and behavioral responses: a fast and efficient testing approach for high-throughput chemical hazard identification. Front. Toxicol. 3 (29) https://doi.org/10.3389/ftox.2021.670496.
Truong, L., Bugel, S.M., Chlebowski, A., Usenko, C.Y., Simonich, M.T., Simonich, S.L., Tanguay, R.L., 2016. Optimizing multi-dimensional high throughput screening using zebrafish. Reprod. Toxicol. 65, 139–147. https://doi.org/10.1016/j.reprotox.2016.05.015.
Truong, L., Reif St, D.M., Mary, L., Geier, M.C., Truong, H.D., Tanguay, R.L., 2014. Multidimensional in vivo hazard assessment using zebrafish. Toxicol. Sci. 137 (1), 212–233. https://doi.org/10.1093/toxsci/kft235.
Truong, L., Tanguay, R.L., 2017. Evaluation of embryotoxicity using the zebrafish model. Methods Mol. Biol. 1641, 325–333. https://doi.org/10.1007/978-1-4939-7172-5_18.
U.S. Food & Drug Administration, 2021. Per- and Polyfluoroalkyl Substances (PFAS). ⟨https://www.fda.gov/food/chemical-contaminants-food/and-polyfluoroalkyl-substances-pfas⟩. (Accessed February 8, 2022).
Ulhaq, M., Carlsson, G., Orn, S., Norrgren, L., 2013. Comparison of developmental toxicity of seven perfluoroalkyl acids to zebrafish embryos. Environ. Toxicol. Pharm. 36 (2), 423–426. https://doi.org/10.1016/j.etap.2013.05.004.
US Environmental Protection Agency (EPA), 2020. Benchmark Dose Software (BMDS) User Guide Version 3.2.
Vogs, C., Johanson, G., Naslund, M., Wulff, S., Sjodin, M., Hellstrandh, M., Lindberg, J., Wincent, E., 2019. Toxicokinetics of perfluorinated alkyl acids influences their toxic potency in the zebrafish embryo (Danio rerio). Environ. Sci. Technol. 53 (7), 3898–3907. https://doi.org/10.1021/acs.est.8b07188.
Wasel, O., Thompson, K.M., Gao, Y., Godfrey, A.E., Gao, J., Mahapatra, C.T., Lee, L.S., Sepúlveda, M.S., Freeman, J.L., 2021. Comparison of zebrafish in vitro and in vivo developmental toxicity assessments of perfluoroalkyl acids (PFAAs). J. Toxicol. Environ. Health A 84 (3), 125–136. https://doi.org/10.1080/15287394.2020.1842272.
Westerfield, M., 2000. The Zebrafish Book. A Guide for the Laboratory Use of Zebrafish (Danio rerio), 4 ed. University of Oregon Press, Eugene.
Westerfield, M., 2007. The Zebrafish Book. A Guide for the Laboratory Use of Zebrafish (Danio rerio), 5th ed. University of Oregon Press, Eugene, Oregon.
Ye, X., Kato, K., Wong, L.Y., Jia, T., Kalathil, A., Latremouille, J., Calafat, A.M., 2018. Per- and polyfluoroalkyl substances in sera from children 3 to 11 years of age participating in the National Health and Nutrition Examination Survey 2013-2014. Int. J. Hyg. Environ. Health 221 (1), 9–16. https://doi.org/10.1016/j.ijheh.2017.09.011.